

Acoustic Multibubble Cavitation in Water: A New Aspect of the Effect of a Rare Gas Atmosphere on Bubble Temperature and Its Relevance to Sonochemistry

Kenji Okitsu,* Takeru Suzuki, Norimichi Takenaka, Hiroshi Bandow, Rokuro Nishimura, and Yasuaki Maeda

Graduate School of Engineering, Osaka Prefecture University, 1-1 Gakuen-cho, Sakai, Osaka 599-8531, Japan

Received: July 20, 2006; In Final Form: September 13, 2006

Acoustic cavitation generates transient microbubbles with extremely high temperatures and high pressures, which can provide unique reaction routes. The maximum bubble temperature attained is widely known to be dependent on the polytropic index and thermal conductivity of the dissolved gas. Here, we show for the first time experimental evidence that the bubble temperature induced by a high frequency ultrasound is almost the same among different rare gases and the chemical efficiency is in proportion to the gas solubility of rare gases, which would be closely related to the number of active bubbles.

Introduction

Acoustic cavitation has seen diverse application in a number of fields, such as synthesis of nanostructured materials,^{1–3} processing of biomass,⁴ sonofusion,⁵ sonodynamic therapy,⁶ and sonochemical degradation of pollutants and hazardous chemicals.^{7,8} Although new applications of acoustic cavitation continue to be developed, the physicochemical properties of the cavitation bubbles, which are transient and locally formed in the liquid, are still unclear. A quantitative and systematic analysis of several parameters, including the bubble temperatures^{9–13} and pressures,¹⁴ number and size distribution of the bubbles,¹⁵ and the behavior and dynamics,¹⁶ is required in order to control the chemical effects of cavitation for application. Active research has been carried out on estimation of the bubble temperature, analyses of sonoluminescence,^{9–12,17} reaction kinetics,^{18–21} and a computer simulation.²² These reports show that the bubble temperatures are in the range between 4000 and 30 000 K, and are dependent on a number of parameters, such as the ultrasonic intensity, frequency, and nature of solvent. It has also been reported that various physical and thermodynamic properties of the dissolved gases (such as the polytropic index, thermal conductivity, and solubility) could influence the bubble temperature and cavitation efficiency.^{23,24}

In sonochemical reactions, a rare gas is often used as the dissolved gas due to its high polytropic index ($C_p/C_v = 1.67$) and chemical inertness; a high C_p/C_v value generates a high temperature²³ and gives a high reaction yield. In addition, it has been reported that the temperature of the collapsing bubbles, the intensity of the sonoluminescence, and the actual chemical efficiency in every case follow the order $\text{He} < \text{Ne} < \text{Ar} < \text{Kr} < \text{Xe}$.^{9,17,25,26} To date, the existence of this order has been thought to be due to the different thermal conductivities of the rare gases, because these gases have the same C_p/C_v value. Although there are many reports concerning the effects of the dissolved gases on the cavitation efficiency,^{3,9,17,20,25,26} quantitative studies are still limited.

We describe here conclusive experimental evidence for the bubble temperature and chemical efficiency of the multibubble

(MB) cavitation induced by 200 kHz ultrasound in an aqueous solution under rare gas atmospheres of He, Ne, Ar, Kr, and Xe. Our report includes a new aspect of the cavitation phenomenon, which is different from many previous reports.

Experimental Details

Ultrasonic irradiation was performed with a 65 mm ϕ oscillator (KAIJO 4021 type, 200 kHz, 200 W). The details of the irradiation setup and the characteristics of the reaction vessel are described elsewhere.³ In short, rare-gas-saturated aqueous solutions of 2-methyl-2-propanol (*t*-BuOH) at concentrations of 1.0, 2.0, 4.0, 6.0, 8.0, and 10.0 mmol L^{–1} were sonicated in a water bath maintained at 20 ± 0.3 °C by a cold water circulation system (TAITEC CL-150R). The bottom of the vessel was made as flat and thin as possible (1 mm), because transmission of the ultrasonic waves increases with decreasing thickness of the bottom. The vessel was mounted at a fixed position relative to the nodal plane of the sound wave (3.8 mm; $\lambda/2$ from the oscillator). The gas products were measured with a GC-FID (SHIMADZU). The bubble temperature was estimated by the sonolysis of aqueous *t*-BuOH in the presence of different rare gases. The cavitation bubble temperatures can be estimated from the distribution of the sonolysis products of C₂H₂, C₂H₄, and C₂H₆. The product ratio (C₂H₂ + C₂H₄)/C₂H₆ is dependent on the bubble temperature, as previously reported.^{18–21} This product ratio is equal to the ratio k_2/k_1 , where k_1 (rate constant for $2\text{CH}_3 \rightarrow \text{C}_2\text{H}_6$) is $2.4 \times 10^{14} \text{ T}^{-0.4} \text{ dm}^3 \text{ mol}^{-1} \text{ s}^{-1}$ and k_2 (rate constant for $2\text{CH}_3 \rightarrow \text{C}_2\text{H}_4 + \text{H}_2$) is $1.0 \times 10^{16} \exp(-134 \text{ kJ/RT}) \text{ dm}^3 \text{ mol}^{-1} \text{ s}^{-1}$. C₂H₂ is formed via the thermal reaction of C₂H₄.

Results and Discussion

Figure 1 shows the estimated bubble temperatures plotted as a function of the thermal conductivity of each rare gas. It is clear that the estimated bubble temperature is almost the same (ca. 3900 K) among all the rare gases. The temperature estimated under argon is also in good agreement with the reported values

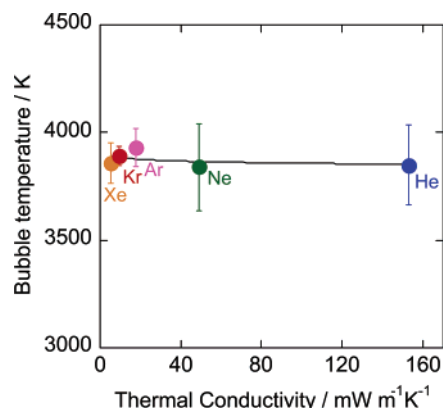


Figure 1. Cavitation bubble temperatures estimated in the presence of different rare gases. Each error bar corresponds to the standard deviation of the measured temperatures ($N = 6$, one sigma).

for aqueous *t*-BuOH (3600 K)¹⁸ and aqueous benzene under an argon atmosphere (4300 K).¹⁰ Until now, it has generally been believed that the bubble temperature and chemical effect of cavitation would be strongly affected by the thermal conductivity of the dissolved gas:^{9,17,25,26} the greater the conductivity of the gas, the more heat would be dissipated to the surroundings, effectively decreasing the bubble temperature. For example, the temperatures estimated from the MB sonoluminescence at 20 kHz in Cr(CO)₆/octanol solution, Xe (5100 K) > Kr (4400 K) > Ar (4300 K) > Ne (4100 K) > He (3800 K), were suggested to be in the same order as the thermal conductivities of the gases.⁹ The experimental data presented here have quite different features from the report of ref 9, namely, the thermal conductivity of the rare gas does not appreciably affect the bubble temperature, as seen in Figure 1. We can reasonably explain our results taking into account the following three factors.

(1) It is known that the bubble collapse time (as well as the bubble lifetime) becomes shorter at higher frequencies. According to the report by Neppiras, the bubble lifetime at 200 kHz ultrasound is about 10 times shorter than that at 20 kHz ultrasound,^{3,23} which in turn is dependent on the size of the cavitation bubble. A relatively high frequency ultrasound is used here, and thus, the collapse of the bubbles would occur by a more adiabatic process because of the rapid collapse. Therefore, it can be suggested that the effect of thermal conductivity on the bubble temperature is negligible compared to that at lower frequency ultrasound. In addition, the resonance bubble radius at 200 kHz ultrasound is about 10 times smaller than that at 20 kHz ultrasound.^{3,23} Since the rate of cooling for larger bubbles will be different from that for small bubbles, it is also suggested that the effect of thermal conductivity may become pronounced in a certain bubble size range.

(2) Suslick et al. reported that the estimated bubble temperature in aqueous solution is lower than those in organic solvents.¹⁰ They suggested that this phenomenon could be attributed to the number of solvent molecules in the cavitation bubbles; that is, larger numbers of solvent molecules in the bubbles result in more endothermic reactions, such as the decomposition of water molecules. In addition to this, the presence of more solvent molecules within the bubbles will also decrease the average polytropic index within the bubbles. Both of the above-mentioned factors would decrease the bubble temperature. In other words, a higher temperature cavitation bubble is generally produced in a solvent with a lower vapor pressure. Considering this point, we propose that the effects of the rare gas property on the bubble temperature should become

less sensitive in aqueous solution than in organic solvents, which have a lower vapor pressure.

(3) We note that the bubble temperatures estimated by sonoluminescence are not comparable with those estimated by the reaction kinetics, because the principle of each estimation method is quite different. This opinion is in accord with a recent report by Ashokkumar and Grieser.²¹ Strictly speaking, the bubble temperature estimated by the sonoluminescence corresponds to the peak temperature which is formed at the core of the collapsing bubbles within a scale of picosecond time.²⁷ On the other hand, the temperatures estimated by the reaction kinetics, such as the temperature dependent reactions of methyl radical recombination,^{18–21} provide average temperatures of the bubble, where the reactions proceed over a longer time scale and a larger volume compared to the sonoluminescence phenomenon. We propose here that the bubble temperature estimated by the reaction kinetics would be a more effective monitor of the chemical efficiency of the cavitation bubbles, because it should represent the actual temperature at which the chemical reactions occur.

It is believed that the chemical effects of the cavitation are dependent on the bubble temperature and follow the order He < Ne < Ar < Kr < Xe. However, our results clearly suggest that the bubble temperature is approximately constant among all of the rare gases.

To provide further support to the above discussion, the cavitation efficiency was evaluated on the basis of the water sonolysis. When an aqueous solution is sonicated, the following reactions occur.

)))



where the symbol))) corresponds to the ultrasonic irradiation. The thermolysis of water molecules occurs due to the high temperatures of the collapsing bubbles.²⁵ OH radicals and H atoms that are formed rapidly recombine to produce H₂O₂, H₂, and H₂O. The yield of H₂O₂ can be related to the yield of OH radicals and hence the cavitation efficiency.^{3,28}

Figure 2a shows the yields of H₂O₂ under different rare gas atmospheres, where the yields are plotted as a function of the thermal conductivity of the rare gases. In the case of each rare gas atmosphere (He, Ne, Ar, Kr, and Xe), it was observed that the yield of H₂O₂ exponentially decreased with increasing thermal conductivity of the gas. The yields are also plotted for He/Xe mixed atmospheres, where the thermal conductivity of each mixed gas is calculated on the basis of the solubility and established method.^{29,30} For example, in an 80:20 He/Xe atmosphere, the ratio of these gases in water corresponds to 23.7:76.3 He/Xe taking into account the solubility of He (mole fraction to water, 7.04×10^{-6})³¹ and Xe (mole fraction to water, 90.5×10^{-6})³¹ in water. The average thermal conductivity of the gas mixture can be estimated to be 23.7 mW m⁻¹ K⁻¹ using values of He (151 mW m⁻¹ K⁻¹)³¹ and Xe (5.62 mW m⁻¹ K⁻¹)³¹ and eq 5 as given below:^{29,30}

$$k_m = 0.5(k_{sm} + k_{rm}) \quad (5)$$

where k_m is the thermal conductivity of a mixture and k_{sm} and

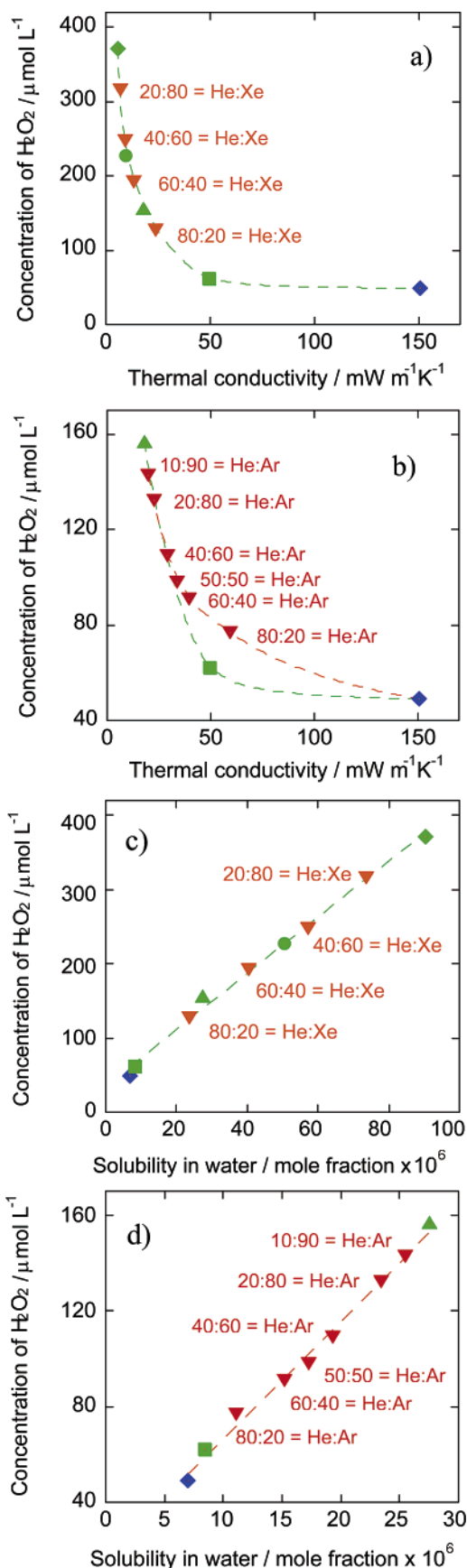


Figure 2. Concentrations of H_2O_2 formed from the sonolysis of pure water as functions of thermal conductivity of rare gases (a and b) and solubility in water (c and d) under various rare gas atmospheres. Conditions: temperature of bulk solution, 20 ± 0.3 °C; irradiation time, 30 min; (blue \blacklozenge), He; (green \blacksquare), Ne; (green \blacktriangle), Ar; (green \bullet), Kr; (green \blacklozenge), Xe; (orange \blacktriangledown), He/Xe mixture; (red \blacktriangledown), He/Ar mixture.

TABLE 1: Solubility and Thermal Conductivity of Rare Gases and Rare Gas Mixtures

atmospheric gas	solubility in water/ mole fraction	gas ratio in water	thermal cond./ $\text{mW m}^{-1} \text{K}^{-1}$
He	7.04×10^{-6} ^a		151 ^b
Ne	8.39×10^{-6} ^a		49.3 ^b
Ar	27.5×10^{-6} ^a		17.9 ^b
Kr	50.4×10^{-6} ^a		9.42 ^b
Xe	90.5×10^{-6} ^a		5.62 ^b
He/Ar = 10:90	25.5×10^{-6} ^c	He/Ar = 2.8:97.2 ^c	20.0 ^d
He/Ar = 20:80	23.4×10^{-6} ^c	He/Ar = 6.0:94.0 ^c	22.4 ^d
He/Ar = 40:60	19.3×10^{-6} ^c	He/Ar = 14.6:85.4 ^c	28.9 ^d
He/Ar = 50:50	17.3×10^{-6} ^c	He/Ar = 20.4:79.6 ^c	33.4 ^d
He/Ar = 60:40	15.2×10^{-6} ^c	He/Ar = 27.8:72.2 ^c	39.3 ^d
He/Ar = 80:20	11.1×10^{-6} ^c	He/Ar = 50.6:49.4 ^c	58.8 ^d
He/Xe = 20:80	73.8×10^{-6} ^c	He/Xe = 1.9: 98.1 ^c	7.06 ^d
He/Xe = 40:60	57.1×10^{-6} ^c	He/Xe = 4.9:95.1 ^c	9.35 ^d
He/Xe = 60:40	40.4×10^{-6} ^c	He/Xe = 10.5:89.5 ^c	13.5 ^d
He/Xe = 80:20	23.7×10^{-6} ^c	He/Xe = 23.7:76.3 ^c	23.7 ^d

^a Estimated on the basis of ref 31 at 293.15 K and 1 atm. ^b Reference 31 at 300 K and 1 atm. ^c Estimated with a linear mixing rule. ^d Estimated on the basis of refs 29 and 30, where the formation of cavitation bubbles with the estimated gas ratio was assumed.

k_{rm} are the mean conductivities based on simple mixing and reciprocal mixing, respectively:

$$k_{\text{sm}} = x_1 k_1 + x_2 k_2 \quad (6)$$

and

$$1/k_{\text{rm}} = x_1/k_1 + x_2/k_2 \quad (7)$$

where x_1 and x_2 are the mole fractions and k_1 and k_2 are the thermal conductivities of each rare gas. The thermal conductivities estimated by eq 5 are summarized in Table 1. In the case of the He/Xe mixture, the same tendency is observed for the two curves in Figure 2a. To get more quantitative information, a He/Ar mixture was used for the atmospheric gas (Figure 2b). Although the yield gradually decreased as the thermal conductivity increased, there appears to be no direct correlation between the thermal conductivity and the H_2O_2 yields. For example, at a thermal conductivity of 40–50 $\text{mW m}^{-1} \text{K}^{-1}$, the Ne atmosphere provides a yield of about 60 $\mu\text{mol L}^{-1}$, whereas the He/Ar atmosphere provides a yield of about 80 $\mu\text{mol L}^{-1}$.

Figure 2c and d shows the H_2O_2 yields plotted as a function of the solubility of the rare gases. A linear dependence between the gas solubility and the H_2O_2 yields can be clearly observed in both pure and mixed rare gases. This result would suggest that the number of cavitation bubbles can be related to the gas solubility. Figure 2c and d also shows that the H_2O_2 yield follows the order $\text{He} < \text{Ne} < \text{Ar} < \text{Kr} < \text{Xe}$. A similar trend has been reported in a previous study²⁵ for the yield of spin-trapped hydroxyl radicals. However, as described above, it should be noted that the bubble temperature is the same among all of the rare gases. Therefore, it is clear that the cavitation efficiency is significantly affected by the amount of dissolved gas in water.

The relationship between the gas solubility and the cavitation efficiency presented here is also applicable to the discussion given in previous reports. For example, Suslick et al. reported the chemical efficiency of hydrodynamic cavitation under Ar/He mixtures,³² where the rate of I^- oxidation decreased exponentially as the thermal conductivity of the dissolved gas increased. If the gas solubility were to be plotted along the x -axis instead of the thermal conductivity, a clear relationship could also be observed between the rate of I^- oxidation and gas solubility.

We propose that, to determine the effects of thermal conductivity and solubility on the cavitation efficiency, both parameters should be plotted, as shown in Figure 2. To our knowledge, no reports have quantitatively measured the effect of the gas solubility on the cavitation efficiency among different rare gases. This may be due to the following reasons: (1) it has been strongly believed that the thermal conductivity would affect the bubble temperature, (2) the actual cavitation efficiency was not investigated quantitatively, and (3) the relationship between the gas solubility and the number of active bubbles has not yet been understood correctly. This paper shows for the first time conclusive experimental evidence that the bubble temperature induced by a high frequency ultrasound is almost the same among different rare gases and the cavitation efficiency is in proportion to the gas solubility of rare gases, which would be closely related to the number of active bubbles.

It is suggested that the chemical effects of MB cavitation in water are the highest in the frequency range 200–500 kHz.^{8,28,33} Hence, the use of high frequency ultrasound should be of significant interest in various research fields and industries. Depending on the irradiation conditions, it is clear that various types of cavitation dynamics need to be considered to explain sonochemical reactions. For example, the gas solubilities in water are much lower than those in organic solvents,³¹ suggesting that the different cavitation dynamics should occur between water and organic solvents.

Acknowledgment. We acknowledge the support from 21st century COE program of JSPS in Japan. We also acknowledge Dr. Y. Nagata and Dr. M. Ashokkumar for their fruitful discussion.

References and Notes

- (1) Suslick, K. S.; Price, G. J. *Annu. Rev. Mater. Sci.* **1999**, 29, 295.
- (2) Bradley, M.; Ashokkumar, M.; Grieser, F. *J. Am. Chem. Soc.* **2003**, 125, 525.
- (3) Okitsu, K.; Yue, A.; Tanabe, S.; Matsumoto, H.; Yobiko, Y.; Yoo, Y. *Bull. Chem. Soc. Jpn.* **2002**, 75, 2289.
- (4) Stavarachea, C.; Vinatoru, M.; Nishimura, R.; Maeda, Y. *Ultrason. Sonochem.* **2005**, 12, 367.
- (5) Taleyarkhan, R. P.; Cho, J. S.; West, C. D.; Lahey, R. T., Jr.; Nigmatulin, R. I.; Block, R. C. *Phys. Rev. E* **2004**, 69, 036109.
- (6) Rosenthal, I.; Sostaric, J. Z.; Riesz, P. *Ultrason. Sonochem.* **2004**, 11, 349.
- (7) Okitsu, K.; Iwasaki, K.; Yobiko, Y.; Bandow, H.; Nishimura, R.; Maeda, Y. *Ultrason. Sonochem.* **2005**, 12, 255.
- (8) Hung, H.-M.; Hoffmann, M. R. *J. Phys. Chem. A* **1999**, 103, 2734.
- (9) McNamara, W. B., III; Didenko, Y. T.; Suslick, K. S. *Nature (London)* **1999**, 401, 772.
- (10) Didenko, Y. T.; McNamara III, W. B.; Suslick, K. S. *J. Am. Chem. Soc.* **1999**, 121, 5817.
- (11) Hilgenfeldt, S.; Grossmann, S.; Lohse, D. *Nature (London)* **1999**, 398, 402.
- (12) Flannigan, D. J.; Suslick, K. S. *Nature (London)* **2005**, 434, 52.
- (13) Camara, C.; Putterman, S.; Kirilov, E. *Phys. Rev. Lett.* **2004**, 92, 124301.
- (14) McNamara, W. B., III; Didenko, Y. T.; Suslick, K. S. *J. Phys. Chem. B* **2003**, 107, 7303.
- (15) Tuziuti, T.; Yasui, K.; Iida, Y. *Ultrason. Sonochem.* **2005**, 12, 73.
- (16) Lauterborn, W.; Kurz, T.; Mettin, R.; Ohl, C. D. *Adv. Chem. Phys.* **1999**, 110, 295.
- (17) Young, F. R. *J. Acoust. Soc. Am.* **1976**, 60, 100.
- (18) Tauber, A.; Mark, G.; Schuchmann, H.-P.; von Sonntag, C. *J. Chem. Soc., Perkin Trans.* **1999**, 2, 1129.
- (19) Hart, E. J.; Fischer, C.-H.; Henglein, A. *Radiat. Phys. Chem.* **1990**, 36, 511.
- (20) Nagata, Y.; Okuno, H.; Mizukoshi, Y.; Maeda, Y. *Chem. Lett.* **2001**, 142.
- (21) Ashokkumar, M.; Grieser, F. J. *Am. Chem. Soc.* **2005**, 127, 5326.
- (22) Yasui, K. *Phys. Rev. E* **2001**, 63, 035301.
- (23) Neppiras, E. A. *Phys. Rep.* **1980**, 61, 159.
- (24) Henglein, A. *Ultrasonics* **1987**, 25, 6.
- (25) Kondo, T.; Gamson, J.; Mitchell, J. B.; Riesz, P. *Int. J. Radiat. Biol.* **1988**, 54, 955.
- (26) Didenko, Y. T.; Pugach, S. P. *Ultrason. Sonochem.* **1994**, 1, S9.
- (27) Bradley, B. P.; Putterman, S. J. *Nature (London)* **1991**, 352, 318.
- (28) Koda, S.; Kimura, T.; Kondo, T.; Mitome, H. *Ultrason. Sonochem.* **2003**, 10, 149.
- (29) Reid, C. R.; Sherwood, K. T. *The properties of gases and liquids*; McGraw-Hill Book Company, Inc.: New York, 1958.
- (30) Brokaw, R. S. *Ind. Eng. Chem.* **1955**, 47, 2398.
- (31) Kagaku Binran, II-66, II-156 (1993), Ed by The Chemical Society of Japan, Maruzen, Japan.
- (32) Suslick, K. S.; Mdleleni, M. M.; Ries, J. T. *J. Am. Chem. Soc.* **1997**, 119, 9303.
- (33) Okitsu, K.; Ashokkumar, M.; Grieser, F. J. *J. Phys. Chem. B* **2005**, 109, 20673.